Analysing a Multi-hop UMTS over multiple Frequency Schemes and an urban Environment

K Konstantinou, M A Imran, C Tzaras
Centre for Communication Systems Research, University of Surrey, Guildford, GU2 7XH, UK
Email: {k.konstantinou, m.imran}@surrey.ac.uk, costas.tzaras@kimatica.com

***Abstract*— In this paper we analyse the performance of a relay based UMTS system in an urban environment using multiple hops on multiple frequency bands. Measurement based path loss, fading and shadowing models are used in the Manhattan grid deployment scenario. Both uplink and downlink operations of the cellular system are considered at the same time. Two hop communication links over the uplink and downlink are operated at four non-overlapping spectrum bands in order to minimise interference. This results in several possible frequency schemes. Power solutions are derived analytically for the selected frequency schemes. The system performance is evaluated both by simulation and analysis and improvement by employing relays is shown.**

***Index Terms*— UMTS, Cellular, Relay, Manhattan Grid.**

I. INTRODUCTION

With the mobile communications technology becoming more and more widespread, urban outdoor environment usually has a high density of idle terminals. It is to the network operators' advantage to harness the omnipresence of these terminals that are capable of communicating. These idle terminals can be used as relays for users which experience unsatisfactory quality of the direct link with the base station. Strategically placed fixed relays, with infinite power-supply and directivity-gain capabilities, can also be deployed for the same end. This establishes a multi-hop communication link, as opposed to the conventional direct communication link. By breaking the link into multiple hops the communication is enabled while transmitting reduced powers, which consequently is translated into lower interference margin in the terminal receivers. As the conventional Code Division Multiple Access system is interference limited, reduction in interference accommodates the service of more users, i.e. improved user-capacity, and for better performance, i.e. coverage extension for high data rate services.

Owing to the potential benefits of relaying, there has been an upsurge of interest in multihop mobile networks. Initially a multihop routing protocol–Opportunity Driven Multiple Access (ODMA)–was considered to be applied to Universal Mobile Telecommunications System (UMTS) Time Division Duplex (TDD) [1]. Revisions of the standard discontinued due to concerns over complexity, battery life of terminals-on-standby, and signalling overhead issues. ODMA capacity investigation was conducted in [2]. Other proposed systems include: an enhanced ad-hoc (Global System for Mobile communications) GSM network [3], a Unified Cellular and Ad-Hoc Network architecture using 802.11-based peer-to-peer links [4], an Integrated Cellular and Ad Hoc Relaying system which dynamically balances the traffic heterogeneity among cells [5], a Multihop Cellular system where every mobile user participates in relaying [6], a UTRA TDD system augmented by Intelligent Relaying capability [7], fixed relay systems [8] – [9], and wired relay systems [10]. The relay routing was researched by [11] and the DownLink (DL) throughput in [12].

In this paper we evaluate the performance of a relay-based UMTS system in an urban environment. We focus on UpLink (UL) capacity while considering the DL transmissions as well. We use fixed (optimally positioned) or mobile relays and an empirical path loss models, suitable for an example urban network laid out on the Manhattan grid. We identify different frequency allocation schemes for allocating frequency on the two hops of communication (source to relay and relay to destination) on two different links: UL and DL. We compare two promising schemes with respect to their power saving, under optimum relay positioning. Optimum relay position is found by an exhaustive search, and to this end, we propose an analytical approach to find the power solution of the whole system for an assumed relay position. Additionally, we assume directional antennas with varying antenna gains at different transceiver nodes and observe the effect of this variation on the optimum relay positions.

We show that the introduction of relays in the UMTS system saves power (as a consequence it generates less interference to other systems as well) and also increases the maximum achievable load factor by 6%. For a more realistic system (shadowing, mobility model, random user distribution, practical transmit power restrictions) we resort system level simulations to show that for a given outage probability relaying can achieve higher load factor.

The rest of the paper is organised as follows. We present the model, deployment scenario, and assumptions in the next section. We identify the frequency allocation schemes and present the motivation to analyse two of them. Section III presents the relevant analysis to find the power solution for a given Base Station (BS), Relay Station (RS) and User Equipment (UE) positions. Selected frequency schemes are compared in section IV and conclusions are discussed in section V.

This paper is an extension of "CDMA Relaying in Multiple Frequency Schemes in a Manhattan Environment," by K. Konstantinou, and C. Tzaras, appeared in 24th IEEE VTC, Baltimore, O. '07. © 2007 IEEE.

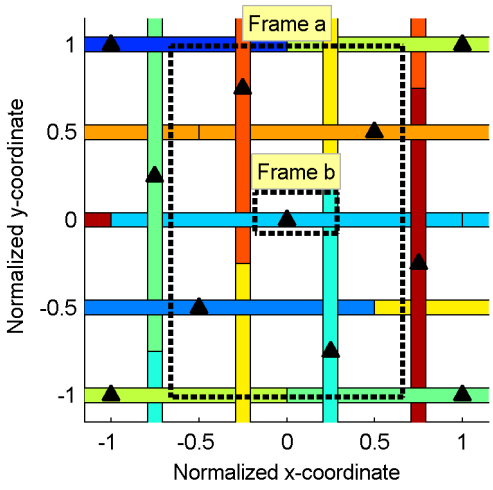

Figure 1. The urban cell overview. The frames refer to Fig. 2 and Fig. 3. The BS locations (triangles) and grid dimensions comply with [14].

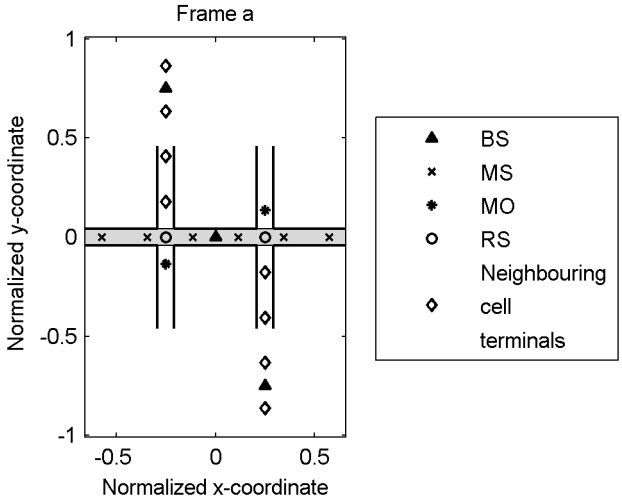

Figure 2. Uniformly distributed terminal positions on the Manhattan grid.

II. Model and Frequency Allocation Schemes

A. System Model Description

The UL of a UMTS Frequency Division Duplex mobile network is considered. Whereas in the conventional, Single-Hop (SH)-only, UMTS system there are two types of terminals, namely BS and UE, in the relay-enhanced UMTS there is a new type: the active repeater transceiver RS. It is imperative that our analysis have a multi-cell nature, in order to take into consideration the potential traffic diversion function of relaying [13]. Therefore, our analysis focuses on a single cell and, by assuming symmetry in the link topology, the multi-cell system is modelled by the introduction of the other-to-own cell interference ratio η. Note herein that, in the case of traffic-diversion relaying, due to the assumed symmetry, there will be equivalently, similar relayed links originating from neighbouring cells routed to the BS of the examined cell.

The selected deployment is the urban Manhattan grid. The urban-cell in this scenario differs fundamentally from the classical circular or hexagonal cell-shape approach. This is due to the cell-extension-along-the-street pattern and the inherent shadowing caused by the corners of the building blocks, creating coverage-holes; see Fig. 1.

Let the Mobiles in Outage (MOs) are the UEs which are opted for multi-hop communication and Mobile Stations (MSs) are the UEs in SH-communication with the BS. We can distinguish the terminals RSs and MOs in accordance to their participation to the two different functions: same-cell and other-cell relaying. However, it has been shown in our previous work [15], that same-cell relaying importance is of lesser extent, so that only other-cell relaying will be considered in the paper analysis. Note that, in the other-cell relaying, the MOs are UEs, which in the conventional UMTS would be serviced by the neighbouring cells, but in the multi-hop UMTS are opted to relay their traffic to the examined cell's BS, via the RS. Fig. 2 plots the different terminals and their positions on an examined cell and its immediate neighbours. The positions of the neighbouring cell terminals are also plotted. The examined cell is shaded. Terminals are assumed to be positioned on a line, in the middle of the road.

Only two MOs are considered per cell, one at either side. The positioning of the two respective RSs was performed by exhaustive search along the line of the main road and side street (inclusive of street corner), seeking to minimise the interference at the BS, thus maximising system capacity [16]. Preserving the symmetry, the RS positions are symmetrical about the BS location.

Each RS is assumed to possess two antennas: one for the BS ($\mathrm{RSant_{LH}}$) and one for the MO links ($\mathrm{RSant_{P2P}}$). In accordance to the RS position (on the main road, at the corner, or inside the side street), each antenna may be considered to have a different radiation pattern. E.g. inside the side-street, the system performance would be benefitted if the peer-to-peer (P2P) antenna featured directivity gain towards the MO, however, at the same RS location, a similar gain-lobe consideration for the Last-Hop (LH) antenna is unimportant; see Fig. 3. The Figure shows the radiation pattern (azimuth) of the two RS antennas, depending on the RS location. The elevation radiation pattern, considered to be of the same shape as in the azimuth, is assumed to have its peak gain towards the BS ($\mathrm{RSant_{LH}}$) or MO ($\mathrm{RSant_{P2P}}$). Note that, when the RSs are positioned on the main road their patterns are facing each other, however, the interference between them is reduced, assuming the elevation-angle difference.

The assumed path loss models, for the SH and relay communication, and several system parameters are summarised in Table I. We choose the WINNER II [17] path loss model, referring specifically to a Manhattan-like grid street-layout. This model and the jointly used P2P model for street-level links [18] are both empirical in nature.

B. Frequency Allocation Schemes

A two-hop system is examined. We assume that, the assumed system uses two pairs of 5MHz channels: two

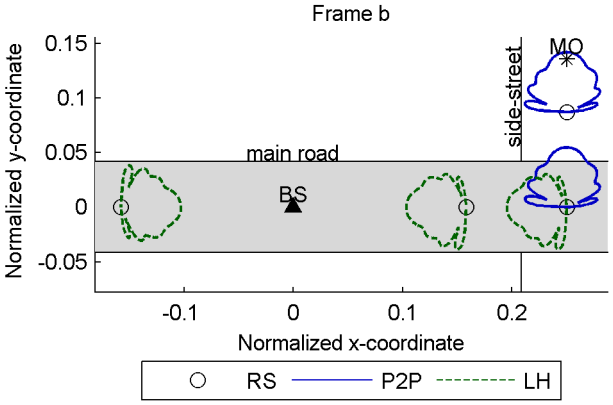

Figure 3. Directivity gain lobes of $\mathrm{RSant}_{\mathrm{LH}}$ and $\mathrm{RSant}_{\mathrm{P2P}}$.

TABLE I.
SYSTEM PARAMETERS. MCL: MINIMUM COUPLING LOSS; SINR: SIGNAL TO INTERFERENCE NOISE RATIO.

Parameter	Value
Inter- to intra-cell ratio η	0.2 [19]
BS/MS Gain	11/0dB (omni) [14]
RS Gain	$\mathrm{Gn}_{\mathrm{RS}} \in (0, 11)$dBi
RS radiation pattern	[20]
BS/RS/MS Height	5/3/1.5m [21]
BS/RS Thermal Noise $N_{\mathrm{BS}}/N_{\mathrm{RS}}/N_{\mathrm{MS}}$	-103/-99/-99dBm [14]
Path Loss Model	SH/LH: [17], P2P: [18]
Effective Height	1.0m [17]
Frequency	2GHz [22]
SINR Target a	dependent on rate r [22]
MCL LH, SH	53dB [14]
MCL P2P	32.4dB($d_{\mathrm{P2P}} = 0.5$m)
Band-Width W	3.840Mcps [22]

UL ($f_1\uparrow$, $f_2\uparrow$) and two DL carriers ($f_1\downarrow$, $f_2\downarrow$), and that both UL bands are used for both SH and multi-hop links. We also assume frequency orthogonality between the hops; the MOs use two carriers (one UL and one DL) for the MO–RS links (P2P), and the other two for the LH links. E.g. the MOs in f1 (MOf1) employ RSs (RSf1) to communicate with the BS, thus forming the P2Pf1 and LHf1 links, each of which may be occurring in either of the f1↑, f2↑, f2↓, or f1↓ carriers; see Table II. Note that, the relay-formed links are denoted by the frequency of the respective MO, not by that of the employed carrier. In the above example, the P2Pf1 and LHf1 links are denoted by f1, although any of them may be occurring in an f2 carrier.

The data channels for duplex relay communication are formed by combinations obtained from the following grid:

SH P2P LH	f1 f2	↑ ↓

Twelve different combinations (data channels) are formed, by combinations of one element from each column. These channels need to be admitted in four system carriers.

In admitting channels in the available carriers there are several link concurrency-restrictions that define avoidance scenarios. The following cases of avoidance are reckoned:

1) Concurrent transmitting and receiving in the same frequency carrier, provided that no interference cancellation at the BS and/or RS is assumed.
2) Serving the sum of users from both frequencies in one carrier, due to capacity limitations at the BS.

Tanking into account the above restrictions, the four SH links can only be accommodated, each, in a different carrier. Having established the SH links in the four carriers, each of the LH links have the choice to be accommodated in two different carriers (e.g. the LHf1↑ in the carrier with SHf1↑ or SHf2↑). Finally, as regards with the P2P links, the accommodation choices are given by example. The P2Pf1↑ has the choice to be accommodated in two different carriers (any carrier, excluding the one being employed by LHf1 links). The P2Pf1↓ can only be accommodated in one carrier (the one which does not accommodate LHf1 or the P2Pf1↓ links). Similarly, the P2Pf2↑ can be accommodated in two different carriers and P2Pd2↓ in one. The different frequency schemes that are produced, are 64 in number. Further restriction in the link accommodation would be to allow only three types of links in each carrier, providing thus relative equality in the link distribution among the carriers, which narrows down the different frequency schemes to 32 cases.

Different frequency schemes alter the interference reception by defining the terminals that are assigned to receive at a particular carrier, so that if, for example a RS is receiving a great deal of interference from nearby SH users in one scheme, changing the frequency allocation the RS may be switched to transmit at the said frequency band, thus shifting the interference to the BS. This is more apparent in Fig. 4, which plots schematically the occurring links between the terminals for two carriers and two frequency schemes (FS1 and FS2). In FS1 the P2P-originating interference at the BS is lower than in the FS2. The interference levels at the RS are also altered between FS1 and FS2, however, calculation of the transmit power levels in the system is required, for adjudicating on which of FS1/FS2, the interference at the RS receiver is less.

The 32 different frequency scenarios can be classified into two broad categories depending on the frequency load-balance and the carrier concurrency of the P2P↑ and LH↑/SH↑ communication links. We indexed the classes:

a) evenly distributed load and concurrent UL,
b) evenly distributed load and non-concurrent UL,
c) uneven load and concurrent UL, and
d) uneven load and non-concurrent UL.

There is a sole frequency scheme in class a: the already referred Frequency Scheme I (or FS1). The same as for class b: Frequency Scheme II (or FS2).

Furthermore, unevenly distributed load can be dealt with frequency-band handover. Therefore, in this paper we will focus on FS1 and FS2); see Fig. 4 and Table II. In Table II the latin numbers I and II denote the two Frequency Schemes. The transmit/receive status (Tx/Rx) of the RS, dictated by the LH connectivity is also provided.

The users are placed at fixed positions, uniformly distributed in the cell. Therefore, with the assumption that

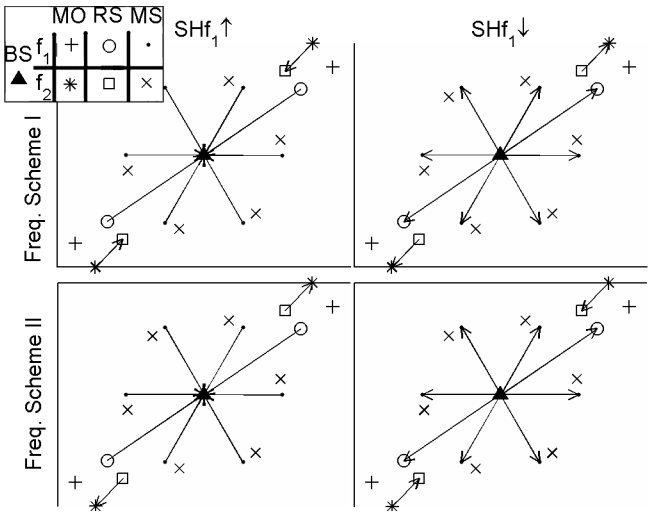

Figure 4. Frequency Schemes I and II.

TABLE II.
ARRANGEMENT OF THE MULTI-HOP UMTS LINKS.

	$f_1\uparrow$	$f_2\uparrow$	$f_2\downarrow$	$f_1\downarrow$
SH	$SHf_1\uparrow$	$SHf_2\uparrow$	$SHf_2\downarrow$	$SHf_1\downarrow$
LH	$LHf_1\uparrow$	$LHf_2\uparrow$	$LHf_2\downarrow$	$LHf_1\downarrow$
RSf_1	Tx	(I) $P2Pf_1\uparrow$ (II) $P2Pf_1\downarrow$	(I) $P2Pf_1\downarrow$ (II) $P2Pf_1\uparrow$	Rx
RSf_2	(I) $P2Pf_2\uparrow$ (II) $P2Pf_2\downarrow$	Tx	Rx	(I) $P2Pf_2\downarrow$ (II) $P2Pf_2\uparrow$

the two frequency bands are equally populated, and that in both bands the terminal positions are matching, the P2P transmissions which are related to the MOs of the second band are coinciding with the P2P links of the MOs pertaining to the first band. This facilitates the analysis, because the powers can be shifted to a single frequency.

The presented analysis is effective for a network operator which deploys in two UMTS frequency bands. However, the analysis is similar to the one if more or a sole frequency band is used. This is because shifting the powers to a single frequency is equivalent to use the same frequency band for P2P, LH and SH links.

III. SYSTEM ANALYSIS

A. Summary of Notation

We represent the total path gain (inclusive of antenna gains) by g, power by p, achieved Signal to Interference plus Noise Ratio (SINR) by a, service bit-rate by r, and an auxiliary parameter by q throughout the paper. The transmitting source is defined on the superscript of the above variables. Especially for the total path gain g we define first the transmitter and then the receiver, separated by a comma. The subscript on the said variables, g, p, and q, denote the index of the superscripted terminals. Particularly for the path gain g, which is defined by a couple of terminals, two indexes are required, written in the same order as the referred superscripted transceivers and separated by a comma. Since the analysis is confined to a single cell, a sole BS exists, and therefore the total path gain g of a link with receiver at BS, requires merely the transmitting source index. Note that, the directivity transceiver gains and the non-reciprocal P2P path loss model, generally maps to $g_{i,j}^{\mathrm{Tx,Rx}} \neq g_{j,i}^{\mathrm{Rx,Tx}}$.

On the other hand, the variables which are associated with the receiver end, i.e. the thermal noise N and the total interference at the receiver I have a single superscript, which defines the receiver type. The subscript refers to the index of the receiver of that type.

B. Transmit Power Solution for the Frequency Scheme II

Equation (1) applies in each link i of the system [22]

$$a_i r_i = \frac{p_i g_i W}{(1+\eta) I_i - p_i g_i + N}, \tag{1}$$

where the superscripts are omitted for equation generality. The calculation of the system transmit powers, of a non-relaying and a relaying network (FS1), was achieved by employing (1), in our previous work [15].

Similar to that analysis, the achieved SINR can be expressed with (1), for every data link of the FS2 multi-hop system. We assume that the number of users in the frequency band is M and that R users are using the relaying function, so that there are R relays in the cell and $M-R$ users are in SH link with the BS. We will assume that the only other-cell relaying interference is existent in the system, as suggested in [15].

Analysing the $f_1\uparrow$ frequency carrier (see Table II), the total received power at the BS, I^{BS}, is given by

$$I^{\mathrm{BS}} = \overbrace{\sum_{j=1}^{M-R} p_j^{\mathrm{MS}} g_j^{\mathrm{MS,BS}}}^{\mathrm{SH}} + \underbrace{\sum_{j=1}^{R} p_j^{\mathrm{RS}\downarrow} g_j^{\mathrm{RSf_2,BS}}}_{\mathrm{P2P}} + \underbrace{\sum_{j=1}^{R} p_j^{\mathrm{RS}\uparrow} g_j^{\mathrm{RSf_1,BS}}}_{\mathrm{LH}}. \tag{2}$$

Similarly, the total received power at each MO_i receiver, namely I_i^{MO}, is given $\forall i = 1,..,R$ by

$$I_i^{\mathrm{MO}} = \overbrace{\sum_{j=1}^{M-R} p_j^{\mathrm{MS}} g_{j,i}^{\mathrm{MS,MO}}}^{\mathrm{SH}} + \underbrace{\sum_{j=1}^{R} p_j^{\mathrm{RS}\downarrow} g_{j,i}^{\mathrm{RSf_2,MO}}}_{\mathrm{P2P}} + \underbrace{\sum_{j=1}^{R} p_j^{\mathrm{RS}\uparrow} g_{j,i}^{\mathrm{RSf_1,MO}}}_{\mathrm{LH}}. \tag{3}$$

We define $\forall i = 1,..,M-R$ and $\forall j = 1,..,M-R$

$$\begin{aligned} A_{i,j} &= \begin{cases} q_j^{\mathrm{MS}} g_j^{\mathrm{MS,BS}} & \text{if } i = j \\ g_j^{\mathrm{MS,BS}} & \text{if } i \neq j \end{cases} \quad \text{and} \\ B_{i,j} &= g_j^{\mathrm{RSf_2,BS}} \\ C_{i,j} &= g_j^{\mathrm{RSf_1,BS}} \\ n_i^{\mathrm{BS,SH}} &= -N_{\mathrm{BS}}/(1+\eta) \end{aligned} \tag{4}$$

$\forall i = 1,..,M-R$ and $\forall j = 1,..,R$. We also define $\forall i = 1,..,R$ and $\forall j = 1,..,M-R$

$$\begin{array}{rll} D_{i,j} & = g_{j,i}^{\mathrm{MS,MO}} & \text{and} \\ E_{i,j} & = \begin{cases} q_j^{\mathrm{RS}\downarrow} g_{j,i}^{\mathrm{RSf_2,MO}} & \text{if } i = j \\ g_{j,i}^{\mathrm{RSf_2,MO}} & \text{if } i \neq j \end{cases} \\ F_{i,j} & = g_{j,i}^{\mathrm{RSf_1,MO}} \\ n_i^{\mathrm{MS}} & = -N_{\mathrm{MS}}/(1+\eta) \end{array} \tag{5}$$

$\forall i,j = 1,..,R$. And finally, $\forall i = 1,..,M-R$ and $\forall j = 1,..,R$, we define

$$\begin{array}{rll} G_{i,j} & = g_j^{\mathrm{MS,BS}} & \text{and} \\ H_{i,j} & = g_j^{\mathrm{RSf_2,BS}} & \\ J_{i,j} & = \begin{cases} q_j^{\mathrm{RS}\uparrow} g_j^{\mathrm{RSf_1,BS}} & \text{if } i = j \\ g_j^{\mathrm{RSf_1,BS}} & \text{if } i \neq j \end{cases} \\ n_i^{\mathrm{BS,LH}} & = -N_{\mathrm{BS}}/(1+\eta) & \end{array} \tag{6}$$

$\forall i,j = 1,..,R$, where

$$\begin{array}{ll} q_i^{\mathrm{MS}} & = 1 - \frac{1+W/(r_i^{\mathrm{MS}} a_i^{\mathrm{MS}})}{1+\eta} \quad , \forall i = 1,..,M-R \\ q_i^{\mathrm{RS}\downarrow} & = 1 - \frac{1+W/(r_i^{\mathrm{RS}\downarrow} a_i^{\mathrm{RS}\downarrow})}{1+\eta} \quad , \forall i = 1,..,R \\ q_i^{\mathrm{RS}\uparrow} & = 1 - \frac{1+W/(r_i^{\mathrm{RS}\uparrow} a_i^{\mathrm{RS}\uparrow})}{1+\eta} \quad , \forall i = 1,..,R. \end{array} \tag{7}$$

Defining

$$\begin{array}{rl} \mathbf{n}_{\mathrm{BS,SH}}^{\mathrm{T}} & = \left(n_1^{\mathrm{BS,SH}},..,n_i^{\mathrm{BS,SH}},..,n_{M-R}^{\mathrm{BS,SH}}\right) \\ \mathbf{n}_{\mathrm{MS}}^{\mathrm{T}} & = \left(n_1^{\mathrm{MS}},..,n_i^{\mathrm{MS}},..,n_R^{\mathrm{MS}}\right) \\ \mathbf{n}_{\mathrm{BS,LH}}^{\mathrm{T}} & = \left(n_1^{\mathrm{BS,LH}},..,n_i^{\mathrm{BS,LH}},..,n_R^{\mathrm{BS,LH}}\right) \end{array} \tag{8}$$

we obtain three sets of linear equations

$$\mathbf{A}\mathbf{p}_{\mathrm{MS}} + \mathbf{B}\mathbf{p}_{\mathrm{RS}\downarrow} + \mathbf{C}\mathbf{p}_{\mathrm{RS}\uparrow} = \mathbf{n}_{\mathrm{BS,SH}} \tag{9}$$

$$\mathbf{D}\mathbf{p}_{\mathrm{MS}} + \mathbf{E}\mathbf{p}_{\mathrm{RS}\downarrow} + \mathbf{F}\mathbf{p}_{\mathrm{RS}\uparrow} = \mathbf{n}_{\mathrm{MS}} \tag{10}$$

$$\mathbf{G}\mathbf{p}_{\mathrm{MS}} + \mathbf{H}\mathbf{p}_{\mathrm{RS}\downarrow} + \mathbf{J}\mathbf{p}_{\mathrm{RS}\uparrow} = \mathbf{n}_{\mathrm{BS,LH}} \tag{11}$$

Solving the system of equations for the transmit powers, $\mathbf{p}_{\mathrm{MS}}$, $\mathbf{p}_{\mathrm{RS}\downarrow}$, and $\mathbf{p}_{\mathrm{RS}\uparrow}$, the only invertible matrices are: $\mathbf{A}$, $\mathbf{E}$, $\mathbf{F}$, and $\mathbf{J}$. Following similar analysis, as in [15], we obtain the solution:

$$\begin{array}{rcl} \mathbf{p}_{\mathrm{RS}\downarrow} & = & \begin{cases} \left[\mathbf{E} - \mathbf{D}\mathbf{A}^{-1}\mathbf{B} + \mathbf{\Phi}\left(\mathbf{G}\mathbf{A}^{-1}\mathbf{B} - \mathbf{H}\right)\right]^{-1} \\ \quad \left[\mathbf{n}_{\mathrm{MS}} - \mathbf{D}\mathbf{A}^{-1}\mathbf{n}_{\mathrm{BS,SH}} + \right. \\ \quad\quad \left. \mathbf{\Phi}\left(\mathbf{G}\mathbf{A}^{-1}\mathbf{n}_{\mathrm{BS,SH}} - \mathbf{n}_{\mathrm{BS,LH}}\right)\right] \end{cases} \\ \mathbf{p}_{\mathrm{RS}\uparrow} & = & \begin{cases} \mathbf{\Upsilon}\left(\mathbf{G}\mathbf{A}^{-1}\mathbf{B} - \mathbf{H}\right)\mathbf{p}_{\mathrm{RS}\downarrow} + \\ \quad \mathbf{\Upsilon}\left(\mathbf{n}_{\mathrm{BS,LH}} - \mathbf{G}\mathbf{A}^{-1}\mathbf{n}_{\mathrm{BS,SH}}\right) \end{cases} \\ \mathbf{p}_{\mathrm{MS}} & = & -\mathbf{A}^{-1}\mathbf{B}\mathbf{p}_{\mathrm{RS}\downarrow} - \mathbf{A}^{-1}\left(\mathbf{C}\mathbf{p}_{\mathrm{RS}\uparrow} - \mathbf{n}_{\mathrm{BS,SH}}\right) \\ \mathbf{\Phi} & = & \left(\mathbf{F} - \mathbf{D}\mathbf{A}^{-1}\mathbf{C}\right)\mathbf{\Upsilon} \\ \mathbf{\Upsilon} & = & \left(\mathbf{J} - \mathbf{G}\mathbf{A}^{-1}\mathbf{C}\right)^{-1} \end{array} \tag{12}$$

where $\mathbf{\Phi}$ and $\mathbf{\Upsilon}$ are auxiliary matrices. However, the transmit power solution given in (12) does not describe the transmit powers of the MOs. These will be inferred by analysing the $\mathrm{f}_1\downarrow$; see Table II.

The total received power at each MS_i receiver, namely I_i^{MS}, is given by

$$I_i^{\mathrm{MS}} = \overbrace{\sum_{j=1}^{M-R} p_j^{\mathrm{BS,SH}} g_{j,i}^{\mathrm{BS,MS}}}^{\mathrm{SH}} + \underbrace{\sum_{j=1}^{R} p_j^{\mathrm{MO}} g_{j,i}^{\mathrm{MO,MS}}}_{\mathrm{P2P}} + \underbrace{\sum_{j=1}^{R} p_j^{\mathrm{BS,LH}} g_{j,i}^{\mathrm{BS,MS}}}_{\mathrm{LH}}. \tag{13}$$

Similarly, the total received power at each RSf_{2i} receiver, namely $I_i^{\mathrm{RSf_2}}$, is given $\forall i = 1,..,R$ by

$$I_i^{\mathrm{RSf_2}} = \overbrace{\sum_{j=1}^{M-R} p_j^{\mathrm{BS,SH}} g_{j,i}^{\mathrm{BS,RSf_2}}}^{\mathrm{SH}} + \underbrace{\sum_{j=1}^{R} p_j^{\mathrm{MO}} g_{j,i}^{\mathrm{MO,RSf_2}}}_{\mathrm{P2P}} + \underbrace{\sum_{j=1}^{R} p_j^{\mathrm{BS,LH}} g_{j,i}^{\mathrm{BS,RSf_2}}}_{\mathrm{LH}}. \tag{14}$$

Likewise, the total received power at each RSf_{1i} receiver, namely $I_i^{\mathrm{RSf_1}}$, is given $\forall i = 1,..,R$ by

$$I_i^{\mathrm{RSf_1}} = \overbrace{\sum_{j=1}^{M-R} p_j^{\mathrm{BS,SH}} g_{j,i}^{\mathrm{BS,RSf_1}}}^{\mathrm{SH}} + \underbrace{\sum_{j=1}^{R} p_j^{\mathrm{MO}} g_{j,i}^{\mathrm{MO,RSf_1}}}_{\mathrm{P2P}} + \underbrace{\sum_{j=1}^{R} p_j^{\mathrm{BS,LH}} g_{j,i}^{\mathrm{BS,RSf_1}}}_{\mathrm{LH}}. \tag{15}$$

We define $\forall i = 1,..,M-R$ and $\forall j = 1,..,M-R$

$$\begin{array}{rll} K_{i,j} & = \begin{cases} q_j^{\mathrm{BS,SH}} g_j^{\mathrm{BS,MS}} & \text{if } i = j \\ g_j^{\mathrm{BS,MS}} & \text{if } i \neq j \end{cases} & \text{and} \\ L_{i,j} & = g_{j,i}^{\mathrm{MO,MS}} & \\ O_{i,j} & = g_j^{\mathrm{BS,MS}} & \end{array} \tag{16}$$

$\forall i = 1,..,M-R$ and $\forall j = 1,..,R$. We also define $\forall i = 1,..,R$ and $\forall j = 1,..,M-R$

$$\begin{array}{rll} P_{i,j} & = g_{j,i}^{\mathrm{BS,RSf_2}} & \text{and} \\ Q_{i,j} & = \begin{cases} q_j^{\mathrm{MO}} g_{j,i}^{\mathrm{MO,RSf_2}} & \text{if } i = j \\ g_{j,i}^{\mathrm{MO,RSf_2}} & \text{if } i \neq j \end{cases} & \\ S_{i,j} & = g_{j,i}^{\mathrm{BS,RSf_2}} & \\ n_i^{\mathrm{RS}} & = -N_{\mathrm{RS}}/(1+\eta) & \end{array} \tag{17}$$

$\forall i,j = 1,..,R$. And finally, $\forall i = 1,..,M-R$ and $\forall j = 1,..,R$, we define

$$\begin{array}{rll} U_{i,j} & = g_j^{\mathrm{BS,RSf_1}} & \text{and} \\ V_{i,j} & = g_j^{\mathrm{MO,RSf_1}} & \\ X_{i,j} & = \begin{cases} q_j^{\mathrm{BS,LH}} g_j^{\mathrm{BS,RSf_1}} & \text{if } i = j \\ g_j^{\mathrm{BS,RSf_1}} & \text{if } i \neq j \end{cases} & \end{array} \tag{18}$$

TABLE III.
SUBSTITUTIONS FOR: $\mathbf{p}_{\mathrm{BS,SH}}$, $\mathbf{p}_{\mathrm{MO}}$, AND $\mathbf{p}_{\mathrm{BS,LH}}$.

substitute	with
$\mathbf{A}$, $\mathbf{B}$, $\mathbf{C}$, $\mathbf{D}$, $\mathbf{E}$, $\mathbf{F}$, $\mathbf{G}$, $\mathbf{H}$, $\mathbf{J}$	$\mathbf{K}$, $\mathbf{L}$, $\mathbf{O}$, $\mathbf{P}$, $\mathbf{Q}$, $\mathbf{S}$, $\mathbf{U}$, $\mathbf{V}$, $\mathbf{X}$
$\mathbf{p}_{\mathrm{MS}}$, $\mathbf{p}_{\mathrm{RS}\downarrow}$, $\mathbf{p}_{\mathrm{RS}\uparrow}$, $\mathbf{n}_{\mathrm{MS}}$	$\mathbf{p}_{\mathrm{BS,SH}}$, $\mathbf{p}_{\mathrm{MO}}$, $\mathbf{p}_{\mathrm{LH}}$, $\mathbf{n}_{\mathrm{RSO}}$

$\forall i, j = 1, .., R$, where

$$\begin{aligned} q_i^{\mathrm{BS,SH}} &= 1 - \frac{1+W/(r_i^{\mathrm{BS,SH}} a_i^{\mathrm{BS,SH}})}{1+\eta} \quad \forall i = 1, .., M-R \\ q_i^{\mathrm{MO}} &= 1 - \frac{1+W/(r_i^{\mathrm{MO}} a_i^{\mathrm{MO}})}{1+\eta} \quad \forall i = 1, .., R \\ q_i^{\mathrm{BS,LH}} &= 1 - \frac{1+W/(r_i^{\mathrm{BS,LH}} a_i^{\mathrm{BS,LH}})}{1+\eta} \quad \forall i = 1, .., R. \end{aligned} \tag{19}$$

Defining $\mathbf{n}_{\mathrm{RS}}^{\mathrm{T}} = \left(n_1^{\mathrm{RS}}, .., n_i^{\mathrm{RS}}, .., n_R^{\mathrm{RS}}\right)$ we obtain three sets of linear equations, from which the three different transmit power vectors can be determined: $\mathbf{p}_{\mathrm{BS,SH}}$, $\mathbf{p}_{\mathrm{MO}}$, and $\mathbf{p}_{\mathrm{BS,LH}}$. The analysis for obtaining the transmit power solution is similar to the already presented, thus it is omitted. The solution is given by (12), by performing the substitutions as summarised in Table III.

Employing (12) and the suggested substitutions, complete knowledge about the system powers is acquired, given the UE locations (path gains) and quality targets.

IV. COMPARISON BETWEEN THE FREQUENCY ALLOCATION SCHEMES

A. Analysis

In the preceded system analysis, uniform user distribution and fixed positions are assumed. However, the location of the RS is not defined, but can be at any position in the centre of the main-road, side-street, or at the corner. The RS position on the overview map alters the RS gain-related matrices which provide with the transmit power solution of the system. Thus, the performance investigation between the two examined frequency allocation schemes, starts with a study on the optimum RS position. The selected criterion for the analysis was to minimise the interference at the BS, as in [16], so as to be compatible with the simulation RS selection algorithm, performed to maximise the predicted overall SINR [23].

Thus, for each frequency allocation scheme, we first obtained the transmit power solution for a number of RS positions, selecting as optimum the one which minimises the interference. Furthermore, as regards to the benefit of the directivity gain at the RS transceiver antenna, different RS antenna gain values were tried.

For simplicity purposes, the same gain values were tried between the antenna employed for links to the BS ($\mathrm{RSant}_{\mathrm{LH}}$) and MOs ($\mathrm{RSant}_{\mathrm{P2P}}$), namely $\mathrm{Gn}_{\mathrm{RS}}$, in the range $\mathrm{Gn}_{\mathrm{RS}} \in (0, 11)$dBi, between the RS patterns being omnidirectional (for $\mathrm{Gn}_{\mathrm{RS}} = 0$dBi) and having equal gain as the BS (11dBi). In order to achieve the required gain values, the radio pattern (acquired from [20]) was scaled down by multiplication with a suitable coefficient.

For each tried gain value, the exploration of the optimum RS position was re-performed, in search of the minimum interference in the system. Fig. 5 plots, in the upper subplot, the range of the system transmit powers, at 68.75% loading-factor, over a range of RS directivity-gain values. The lower subplot shows the respective optimal RS position inside the side-street (lateral distance). The transmit power solution and RS position for the case when both RS antennas are omnidirectional ($\mathrm{Gn}_{\mathrm{RS}} = 0$dBi) is also plotted with markers, in both subplots. The power range is provided with the minimum (min), maximum (max), and median (med) values. Only the UE (MSs and MOs) UL powers are considered, for two reasons: fair comparison between non-relaying (NR) and relaying systems, and because the fixed RSs can be thought as active repeaters connected to the power grid. The transmit powers in the system are piloted for the three following cases: NR, relaying with FS1 and FS2.

When no directivity-gain is considered, FS1 provides a power solution which features narrower range of values between the minimum and maximum, compared to FS2. This is a desirable feature, because it raises the probability of all transmit powers lying within the constraints. The RS positioning is also different between the schemes: in FS1, the RS is best-positioned at the street corner, whereas, in FS2, deep inside the side-street. This is most probably because in FS2, the additional relay interference caused by $\mathrm{P2Pf}_2\downarrow$ link, at the BS receiver, is originating from the RS which is situated closer to the BS, whereas in FS1, the relay interference originator is the MO, which has a bad channel with the BS. The introduction of directivity-gain alters the power solution and RS optimum-positioning. The directivity isolates the BS receiver from the relay-related interference, so that both schemes perform, in terms of average and maximum power, in a similar fashion. The RS positioning is also relatively the same between the two schemes, and inside the side-street. This is the optimum position for several reasons: the MO-RS link is in a good channel which is also reinforced by the directivity gain, the RS-BS link is in a good channel owing to the BS antenna gain and height, the relay-interference is isolated within the side-street and at a very low level. Furthermore, the minimum power is different between the two schemes for the same $\mathrm{Gn}_{\mathrm{RS}}$ value.

Fig. 6 plots the range of the same transmit powers over a range of system loading factors, for three different cases: NR, relaying with FS1 and FS2. This Figure corresponds to $\mathrm{Gn}_{\mathrm{RS}} = 11$dBi, and RS optimally positioned. Both frequency schemes are implemented with lower transmit powers than those involved in the NR case, among all system-loading levels. Higher power reduction is achieved at low transmit-powers, which is more evident in high load-factors, and is suggestive of potency in increasing the data-rate of the respective links. This potential increase in spectral efficiency is also slenderly apparent, since the relaying power solution curves extend further in higher loading-factors than the NR counterpart: 6% increase in the maximum achievable load-factor was calculated for 8 users of equal data-rate. FS1 and FS2 coincide in the median curve. Non-concurrency in UL is shown to aggravate the system performance, compared to FS1.

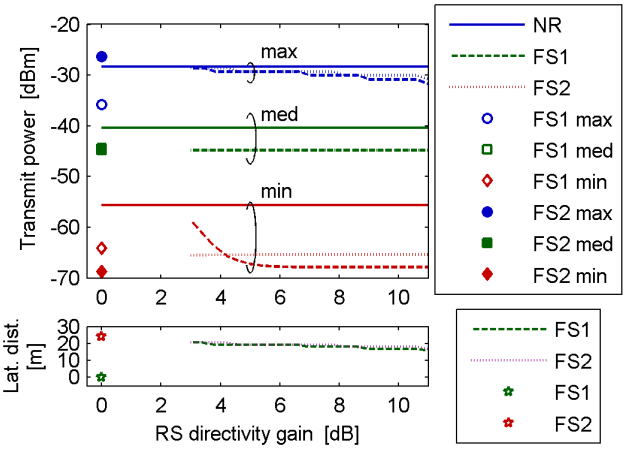

Figure 5. Range of system powers in FS1 and FS2 over RS gain values.

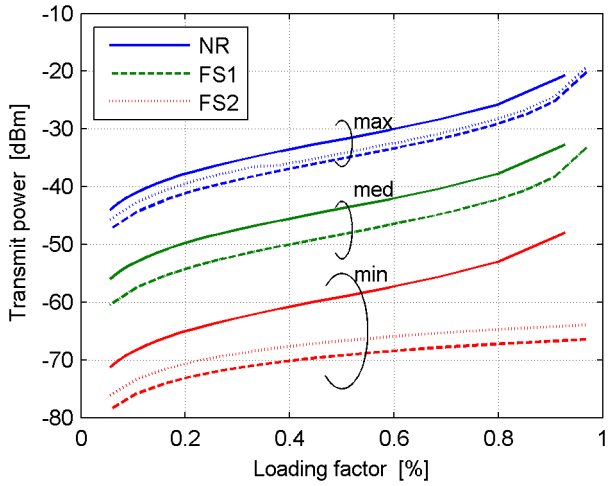

Figure 6. Range of the system powers in FS1, FS2, and NR cases.

B. Simulation

The assumptions presented in the analysis, map to a system which lacks realism. This is because, several propagation and realistic features (shadowing, transmit power limitations, user-mobility, multi-cell deployment, etc.) were simplified or ignored. In our endeavour to amend in realism, the above realistic assumptions dictated directing our interest in developing a system-level simulation to include their effect on evaluating the system performance. This subsection, firstly, discusses the effect of introducing transmit power restrictions, and, in succession, presents the system improvement by employing the relaying technology, over the NR case.

The transmit power limitations [14] are imposed to convey the powers within practical boundaries: the maximum limit is enforced due to health considerations, and the lower limit is imposed so as to prevent communication sources in good channels from transmitting in very low power (technology limitation). The power limitations, if included in the analysis, renders the power solution endeavour, to a bounded minimisation problem. The explicit expression of the minimisation problem is: define the set

TABLE IV.
ANALYSIS AND SIMULATION CONSIDERATIONS. MAX: MAXIMUM; ESTIM.: ESTIMATION

	Analysis	Simulation
Power restrictions	Minimisation problem	✓
Shadowing	Inherent only, otherwise random process	✓
Directivity gain	✓	Not considered
RS positioning	By trial	Max SINR estim.
User distribution	Uniform (fixed)	Uniform (random)
User mobility	None	Pedestrian

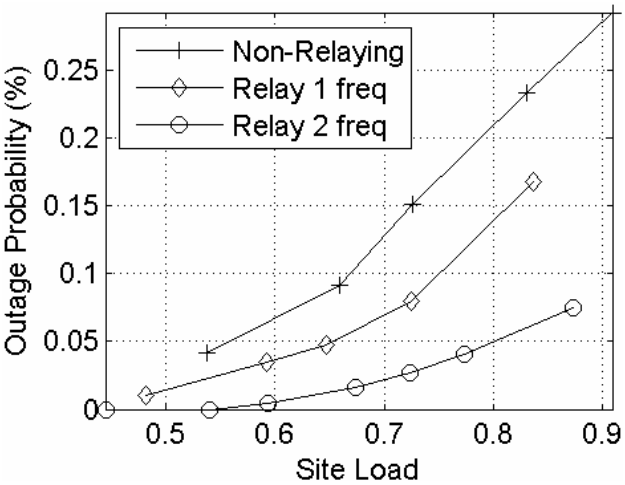

Figure 7. System improvement in terms of outage probability.

of minimum system transmit-powers, each of which lies within the power boundaries and satisfies the link-quality criteria. However, the solution to the stated problem may not always be realisable, when some of the equations (12) are not satisfied. This occurs for higher system loading values, where the MSs closer to the cell-edge are required to transmit at higher level than the permitted in order to preserve the rate of service. Table IV summarises some of the assumptions considered in the analysis and simulation.

The dynamic, multicellular, system-level simulation that we developed for mobile or fixed relays, enabled us to exercise all frequency allocation schemes for their evaluation. The simulation model and a list of its key parameters are provided in our previous work [23]. The main output of the simulation is the outage probability, i.e. the probability that the recorded-SINR is below a threshold-SINR level, which is plotted in Fig. 7 over a range of system loading-factors, for the following three cases depending on the number of relay-enhanced frequency-bands: no band with multihop capabilities (Non-Relaying), relaying only in f1 band (Relay 1 freq), and relaying in both f1 and f2 bands (Relay 2 freq). For 5% outage probability the capacity of the system increases by 50%.

The additional realism alters profoundly the transmit power solution between analysis and simulation. This is mainly because the powers are constrained within limits, drifting all levels towards the same direction. Additionally, the statistical shadowing creates opportunities of

great power reduction, by choosing good-quality relay-links over the deeply-shadowed direct path.

Further work may involve reforming the system equations to find the maximum achievable system sum-rate.

V. Conclusion

We use simulation and analytical approach to validate the potential benefits of using relays in the UMTS system. It is observed that relays (positioned at optimal fixed locations) can reduce the transmit power required to serve the same users in the system. Moreover, the system with relays exhibit a higher maximum load factor as compared to the system with no relaying option. An analytical model with basic assumptions is used for calculating the total transmit power for the system using closed form equations. A more detailed model is used in a system level simulation, with abundant mobile relays, to verify the performance improvement.

Acknowledgment

We thank Ch.Exec.Editor G.J.Sun, for his interest in our research and the reviewers for their valuable comments.

References

[1] Salbu Research and Development (Proprietary) Ltd, "Adaptive communication system," 1978, SA Patent.
[2] T. Rouse, I. Band, and S. McLaughlin, "Capacity and power investigation of opportunity driven multiple access (ODMA) networks in TDD-CDMA based systems," *ICC*, vol. 5, pp. 3202–06, 2002.
[3] G. N. Aggelou and R. Tafazolli, "On the relaying capability of next-generation GSM cellular networks," *IEEE Personal Communications*, vol. 8, no. 1, pp. 40–7, Feb 2001.
[4] H. Luo, R. Ramjee, P. Sinha, L. E. Li, and S. Lu, "UCAN: a unified cellular and ad-hoc network architecture," in *MobiCom*, 2003, pp. 353–67.
[5] C. Qiao and H. Wu, "iCAR: an integrated cellular and ad-hoc relay system," *ICCCN*, pp. 154–61, 2000.
[6] Y.-D. Lin and Y.-C. Hsu, "Multihop cellular: a new architecture for wireless communications," in *INFOCOM*, vol. 3, Mar 2000, pp. 1273–82.
[7] T. Harrold and A. Nix, "Intelligent relaying for future personal communication systems," in *IEE Colloquium on Capacity and Range Enhancement Techniques for the Third Generation Mobile Communications and Beyond*, 2000, pp. 9/1–9/5.
[8] N. Esseling, B. Walke, and R. Pabst, "Performance evaluation of a fixed relay concept for next generation wireless systems," in *PIMRC*, vol. 2, Sept 2004, pp. 744–51.
[9] Y. Yamao, T. Otsu, A. Fujiwara, H. Murata, and S. Yoshida, "Multi-hop radio access cellular concept for fourth-generation mobile communications system," in *PIMRC*, vol. 1, Sept 2002, pp. 59–63 vol.1.
[10] R. Hasegawa, M. Shirakabe, R. Esmailzadeh, and M. Nakagawa, "Downlink performance of a CDMA system with distributed base station," in *VTC Fall*, vol. 2, Oct 2003, pp. 882–6.
[11] V. Sreng, H. Yanikomeroglu, and D. Falconer, "Coverage enhancement through two-hop relaying in cellular radio systems," in *WCNC*, vol. 2, Mar 2002, pp. 881–5.
[12] J. Cho and Z. Haas, "On the throughput enhancement of the downstream channel in cellular radio networks through multihop relaying," *IEEE Journal on Selected Areas in Communications*, vol. 22, no. 7, pp. 1206–19, Sept 2004.
[13] H. Wu, C. Qiao, S. De, and O. Tonguz, "Integrated cellular and ad hoc relaying systems: iCAR," *IEEE Journal on Selected Areas in Communications*, vol. 19, no. 10, pp. 2105–15, Oct 2001.
[14] "ETSI.TR 125 942 v6.3.0 Universal Mobile Telecommunications System (UMTS); RF system scenarios," Tech. Rep., June 2004.
[15] K. Konstantinou, M. Imran, and C. Tzaras, "Transmit power formulation for relay-enhanced UMTS using simulation and theory," under review.
[16] K. Yamamoto and S. Yoshida, "Analysis of reverse link capacity enhancement for CDMA cellular systems using two-hop relaying," *IEICE Trans. Fundamentals*, vol. E87-A, no. 10, pp. 159–163, July 2004.
[17] IST-4-027756 WINNER II, "WINNER II channel models," Tech. Rep., Nov. 2007.
[18] K. Konstantinou, S. Kang, and C. Tzaras, "A measurement-based model for mobile-to-mobile UMTS links," in *VTC Spring*, April 2007, pp. 529–533.
[19] C. Dou, "The maximum available radio resource of a WCDMA downlink," *IEICE Trans. Commun.*, vol. E88B, no. NO.11, pp. 4309–4316, November 2005.
[20] E. Moldovan, "Dual polarized antenna with high directivity for base station antennas," Royal Institute of Technology, S-100 44 Stockholm, Tech. Rep. IRSBEX0406, Feb 2004.
[21] S. R. Saunders and S. R. Simon, *Antennas and Propagation for Wireless Communication Systems*. New York, NY, USA: John Wiley Sons, Inc., 1999.
[22] H. Holma and A. Toskala, Eds., *WCDMA for UMTS*. New York, NY, USA: John Wiley Sons, Inc., 2002.
[23] K. Konstantinou and C. Tzaras, "CDMA relaying in multiple frequency schemes in a manhattan environment," in *VTC Fall*, Sept.-Oct. 2007, pp. 51–5.

Konstantios Konstantinou is a Ph.D. candidate at Unv. of Surrey, UK. He is a M.Eng. from Aristotle Unv. of Thessaloniki (2004) and C.Eng. (Technical Chamber of Greece) in Electrical Engineering & Computer Science, specialised in Comm. He is currently employed by Real Wireless, providing independent consultancy for the wireless industry. His research interests include multihop and 4G systems, and channel modelling.

Muhammad Imran received his Ph.D. (2007) and M.Sc. (2002) degrees from Imperial College London. He has received several national awards in Pakistan, for his academic achievements. In UK, he received Overseas Research Studentship and Imperial College bursary for his Ph.D. studies. He is currently a Research Fellow at Centre for Comm. Systems Research, Unv. of Surrey, UK. His research interests include comm. and information theory, channel coding and signal processing for comm. systems.

Costas Tzaras received the B.Sc. in Physics from the Unv. of Thessaloniki, Greece and the M.Sc. and Ph.D. degrees in Mobile and Satellite Comm. from the Unv. of Surrey, UK. In 1997, he worked as a Research Fellow at the Unv. of Surrey and later he was employed by Vodafone R&D in the Radio Modelling Group to act as the Principal Investigator in radio modelling issues across the Vodafone Group. In 2002, he returned to the Unv. of Surrey as a Lecturer in Mobile Comm. and he continued to lead the Antennas and Propagation Team at Vodafone Global. He is currently employed by Kimatica, a company that specialises in radio planning solutions for the wireless industry. His main interests lie in the field of wireless technology with emphasis on radio channel modelling, network planning and optimisation and capacity investigations on wireless systems.